Low-Cycle Variable Amplitude Fatigue Modeling of Top-and-Seat Angle Connections

JOHN B. MANDER, GOKHAN PEKCAN, and STUART S. CHEN

ABSTRACT

A set of variable amplitude tests was performed on a commonly used type of semi-rigid connection: the top-and-seat angle. Variable amplitude tests included incremental-decremental and step tests to investigate the sequence effects on cyclic and low-cycle fatigue behavior for this class of beam-column connection. The concept of an effective equi-amplitude plastic rotation is introduced as the characteristic measure of rotation history. It is shown that effective rotation is independent of load path when compared to companion constant amplitude test results.[1] An energy based cumulative damage model is characterized in terms of energy-life and energy-rotation relationships. The proposed damage model is employed in fatigue damage prediction analysis and compared with the classical Miner's linear damage accumulation model coupled with the rainflow cycle counting method. The proposed energy based damage model implicitly incorporates the memory effects of the previous loading history and precludes the necessity of performing explicit cycle counting, and it is easily implemented into non-linear time-history analysis for seismic design and evaluation purposes.

INTRODUCTION

During strong earthquakes, structural frames are expected to be subjected to large lateral load reversals. Consequently, relatively large *inelastic* cyclic rotations can be expected in the connections. These rotations can have a pronounced effect on the overall behavior of the frames and on their dynamic response and primarily involve energy dissipation due to the plastic deformation in the connection elements. As a result of cyclic inelastic rotations the connections may fail due to low-cycle fatigue. The ability of the connection to dissipate energy will depend on the connection's capacity to withstand low-cycle fatigue during seismic response.

John B. Mander is assistant professor with the department of civil engineering, State University of New York at Buffalo, NY.

Gokhan Pekcan is graduate research assistant with the department of civil engineering, State University of New York at Buffalo, NY.

Stuart S. Chen is assistant professor with the department of civil engineering, State University of New York at Buffalo, NY.

In experimental low-cycle fatigue studies, fatigue life is commonly expressed as a function of the total and/or plastic strain. If the strain at critical locations in a structural element could be measured, then in conjunction with a suitable cycle counting method and an appropriate S-N type of fatigue model, the fatigue life under random cyclic loading could be predicted. However, structural elements are rather complex systems, and it is not practical and indeed generally impossible to make strain measurements at the critical locations of a connection. Therefore, plastic connection rotations have been used instead and various analysis methods have been developed based on equi-amplitude tests[1] for prediction of low-cycle fatigue performance (damage accumulation) under realistic random histories.

Independently, Palmgren[2] and Miner[3] were first to propose such an analysis method which employs the linear damage accumulation hypothesis commonly known today as Miner's Rule. In this method, estimation of cumulative damage of a component involves converting a random load history into an equivalent sum of cycles by a cycle counting method which is employed in fatigue relationships derived later. Previous investigators such as Krawinkler and Zohrei[4] have applied Miner's Rule for welded steel connections under constant and variable cyclic loading. The difficulty in employing this method with variable amplitude loading arises from the fact that for random loadings such as seismic events, wind, or traffic, cycles are not well-defined. To overcome the irregularities of real load histories, several cycle counting methods have been developed. The rainflow cycle counting technique developed by Matsuishi and Endo[5] is one of the most commonly used cycle counting methods in Miner's Rule applications. This method consists of converting an irregular loading history composed of variable amplitudes into a set of blocks of equivalent harmonic amplitudes.

The present paper describes an incremental-energy based damage modeling approach for predicting fatigue failure of top-and-seat angle semi-rigid connections. This method is able to avoid cycle counting and has the ability to account for path dependency (memory) effects.

EXPERIMENTAL PROGRAM AND TEST RESULTS

Following the constant amplitude tests described in a companion paper[1] several identical specimens were tested under

variable amplitude displacement histories. The test setup consisted of a reaction frame supporting an actuator. The column section (W8×31) was seated on the strong floor, and the beam section (W8×21) was mounted on the column flange and connected to the actuator with a 51-in. moment arm to the column flange. A Unistrut reference frame bolted to the column ends was used to measure drift and also to provide the external control for the hydraulic actuator. Connections contained L6×4×$\frac{3}{8}$ top-and-seat angles of A36 steel bolted to the beam and column flanges, with a 1-in. thick column flange plate to minimize the column flange distortion. For the first two constant amplitude tests[1] load indicator washers were used under the nut along with flat hardened washers. It was observed that proper bolt tensioning required tightening torques of approximately 450 ft-lbs. Therefore, in the rest of the testing program, only A325 hardened flat washers were used with installation torques of 450 ft-lbs. This was considered to apply proper bolt tensioning, as no slip was observed to occur in any of the tests. Connection geometry and test setup are shown in Figure 1.

Three specimens were subjected to step histories in which the connection was initially cycled at a certain drift for a specified number of cycles. After this, the amount of drift was either increased or decreased and the test was resumed at the new drift until the complete fatigue fracture failure occurred. Two specimens were tested under sinusoidally increasing or decreasing displacement amplitudes. A summary of test results is reported in Table 1. Selected hysteresis loops are plotted in Figures 2 through 6.

One of the specimens (V_16) was subjected to low-to-high constant amplitude displacement blocks; first ±2 percent drift for 50 cycles and then ±4 percent drift until complete fatigue fracture failure, for a total of 58 cycles (Figure 2). Specimens V_17 and V_18 were tested under high-to-low constant amplitude displacement blocks. V_17 was first subjected to ±4 percent drift for 8 cycles after which it sustained 173 cycles at ±2 percent drift before failure (Figure 3). V_18 was tested under three different displacement blocks; first ±4 percent drift for 5 cycles, then ±3 percent drift for 10 cycles, and finally ±2 percent drift to failure. Fatigue fracture failure occurred during the 150th cycle at ±2 percent drift (Figure 4). For these tests the number of applied cycles for the initial displacement blocks was chosen to consume approximately half the estimated life based on the range of rotation observed from the equi-amplitude tests.[1]

Finally, specimens V_14 and V_15 were subjected to sinusoidally increasing or decreasing displacement amplitudes between 0 percent and 4 percent in 20 cycles with a cycling frequency of 0.1 Hz. Specimen V_14 was tested by varying the drift amplitude initially from 0 percent to 4 percent. Incipient failure, which was defined as when the first surface crack was visible, was observed at the 60th cycle and fatigue fracture failure at the 64th cycle (Figure 5). Specimen V_15, however, was subjected to initially decreasing drift amplitudes. The first surface crack was visually observable

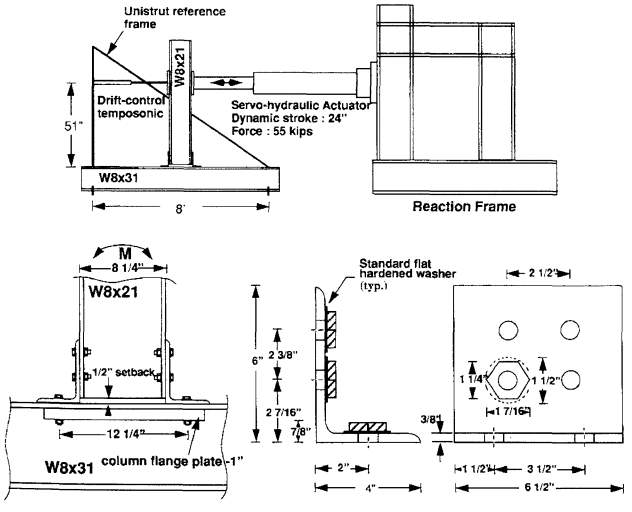

Fig. 1. Test setup and connection geometry.

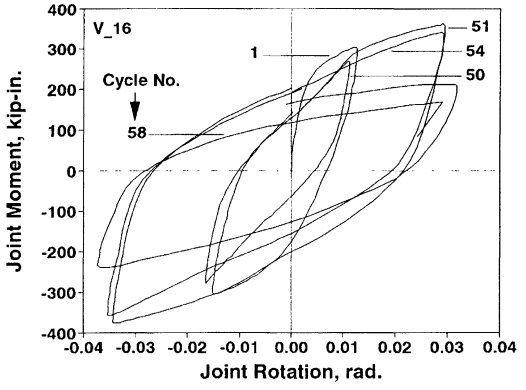

Fig. 2. Moment-rotation graph for the step-test at ±2 percent, ±4 percent drift specimen V_16.

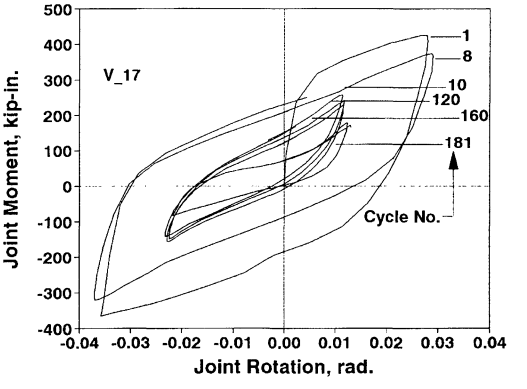

Fig. 3. Moment-rotation graph for the step-test at ±4 percent, ±2 percent drift specimen V_17.

after the 46th cycle, and failure occurred at the 75th cycle (Figure 6).

LOW-CYCLE FATIGUE MODELING

An energy based fatigue damage model is developed herein and applied to the variable amplitude fatigue tests. The model utilizes the fatigue relationships which were derived based on the linearized (log-log) regression analysis of the companion constant amplitude test results[1] plotted on Figure 7 and summarized as follows:

$$\theta_{jp} = 0.0700(2N_f)^{-0.333} \quad (1)$$

$$\theta_{jp} = 0.0849(2N_{ff})^{-0.333} \quad (2)$$

where

θ_{jp} = the plastic rotation of the top and seat angle connection
N_f = the number of cycles to incipient failure and
N_{ff} = the number of cycles to final fatigue fracture.

Energy based fatigue relationships had the following form:

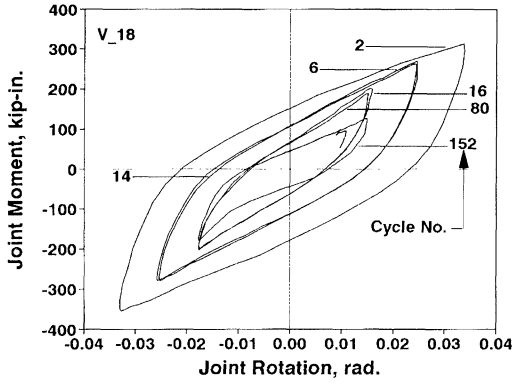

Fig. 4. Moment-rotation graph for the step-test at ±4 percent, ±3 percent, ±2 percent drift specimen V_18.

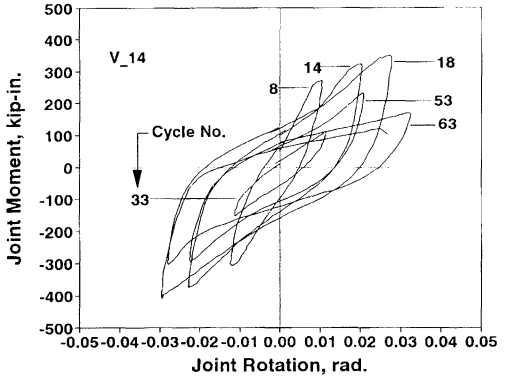

Fig. 5. Moment-rotation graph for the incremental-decremental test ±0 to 4 percent drift specimen V_14.

$$W_f = 0.1440M_{jp}(2N_f)^{0.5} \quad (3)$$

$$W_{ff} = 0.1690M_{jp}(2N_{ff})^{0.5} \quad (4)$$

where

M_{jp} = plastic moment capacity of the connection, and
W_f and W_{ff} = the work done at incipient failure and final fatigue fracture, respectively.

Shown on Figure 8 are the relationships that relate plastic rotation to the energy absorption capacity either at incipient failure or at final fracture:

$$W_f = 0.0151M_{jp}(\theta_{jp})^{-1.0} \quad (5)$$

$$W_{ff} = 0.0229M_{jp}(\theta_{jp})^{-1.0} \quad (6)$$

Also shown in Figures 7 and 8 are variable amplitude data points which will be discussed later.

The proposed energy based fatigue model is compared with the more traditional fatigue model: Miner's Rule coupled with the rainflow cycle counting technique. In what follows, the traditional approach is outlined and then extended to an energy based model that uses the concept of *effective rotation*.

3.1 Miner's Rule

The application of the linear cumulative damage model consists of converting random cycles (displacement histories) into an equivalent number of constant amplitude cycles. Hence, damage fractions due to each individual cycle are summed until fracture occurs. In other words, the damage fraction D_i for the i^{th} cycle is defined as the life used up by the i^{th} event. Failure is assumed to occur when these damage fractions sum up to or exceed unity,

$$D_T = \Sigma D_i = \Sigma \left(\frac{1}{N_f}\right)_i \geq 1 \quad (7)$$

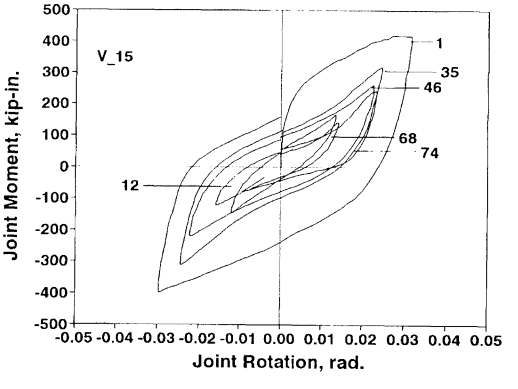

Fig. 6. Moment-rotation graph for the decremental-incremental test ±4 to 0 percent drift specimen V_15.

Table 1.
Specific Tests Results

Spec Id.	% Drift	Cyc. #	Range of Connection Rotation (rad)	Area of Single Hysteresis Loop (kip-in)	Cumulative Area of Hysteresis Loops (kip-in)
V_14	1.69	8	0.0196	2.44	6.67
	2.75	14	0.0397	8.42	40.8
	1.53	33	0.0260	1.85	224.9
	2.55	53	0.0405	5.73	253.2
	3.57	63	0.0604	10.2	375.0
V_15	3.96	1	0.0614	20.2	20.22
	2.95	6	0.0462	8.23	78.02
	1.93	12	0.0317	2.53	105.9
	2.13	68	0.0366	1.46	119.0
	1.97	74	0.0329	4.54	341.7
V_16	2	1	0.0272	6.29	6.29
		50	0.0275	4.68	234.8
	4	51	0.0638	20.9	255.7
		58	0.0695	16.0	393.6
V_17	4	1	0.0644	21.2	21.20
		8	0.0661	17.3	148.3
	2	9	0.0346	5.67	154.0
		181	0.0357	2.35	781.5
V_18	4	1	0.0740	23.0	23.00
		5	0.0580	11.8	96.06
	3	6	0.0500	9.41	105.5
		14	0.0502	9.36	180.2
	2	15	0.0413	5.78	185.9
		152	0.0286	1.20	646.6

where

D_i = $(1/N_f)_i$ is the damage fraction for the i^{th} cycle and

$(N_f)_i$ = fatigue life at rotation amplitude θ_{ji}.

Miner's Rule can be modified as follows,

$$D_{wT} = \Sigma D_{wi} = \Sigma \left(\frac{w_i}{W_{fi}} \right) \geq 1 \qquad (8)$$

in which

w_i = total work done (energy dissipated) for the i^{th} *cycle* at the current rotation amplitude θ_{ji} and

W_{fi} = total work done as a function of θ_{ji}.

The value of W_{fi} can be calculated from the energy vs. total and/or plastic rotation amplitude relationships obtained previously. The experimental data was evaluated using Miner's rule and reported in Table 2.

3.2 Effective Rotation

By employing Miner's Rule, an effective (or equivalent) constant amplitude rotation can be derived for a variable amplitude history. The linear log-log relationship of plastic rotation to the number of reversals ($2N_f$) was first developed by Coffin[6] and Manson.[7] Later Koh and Stephens[8] suggested that total rotation amplitude could be used instead of plastic rotation as follows,

$$N_f = C\theta_j^{1/c} \qquad (9)$$

where

C = fatigue ductility coefficient and
c = fatigue ductility exponent.

The damage fraction D_i according to Miner's Rule, for the i^{th} cycle of loading, can be expressed as $D_i = 1/N_f$ where N_f is given by Equation 9 for a certain rotation amplitude. Total damage, therefore, can be written as in Equation 7,

$$D_T = \Sigma D_i = \Sigma \left(\frac{1}{N_f} \right)_i = \Sigma \left(\frac{1}{C\theta_j^{1/c}} \right)_i \qquad (10$$

Damage at incipient failure, for N_f cycles at effective rotation amplitude, $\theta_{j\,eff}$ is given by

$$D_{constant} = N_f \left(\frac{1}{C\theta_{j\,eff}^{\,1/c}} \right) = 1 \tag{11}$$

Equivalent amplitude can be determined by equating the total damage due to random loading to that due to constant-equivalent amplitudes (Equation 11), which yields the following relation:

$$\frac{D_{random}}{D_{constant}} = \frac{\sum_{i=1}^{N_f} (\theta_j^{-1/c})_i}{N_f \theta_{j\,eff}^{\,-1/c}} = 1 \tag{12}$$

Solving Equation 12 for $\theta_{j\,eff}$ gives

$$\theta_{j\,eff} = \left(\frac{1}{N_f} \sum_{1}^{N_f} \theta_j^{-1/c} \right)^{-c} \tag{13}$$

Then effective plastic equi-amplitude rotation (assuming $R = -1$) can be defined as

$$\theta_{jp\,eff} = \theta_{j\,eff} - \frac{M(\theta_{j\,eff})}{K_e} \tag{14}$$

where

$\theta_{j\,eff}$ = effective rotation amplitude determined from Equation 13 for the entire history,

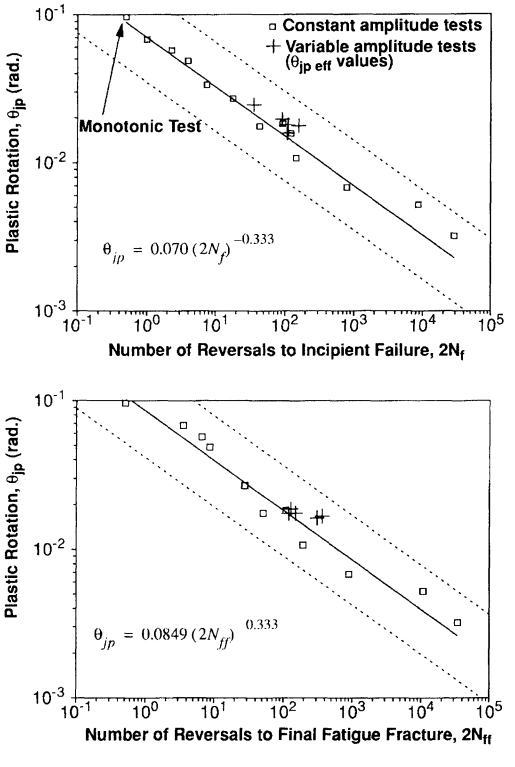

Fig. 7. (a) Plastic rotation vs N_f. (b) Plastic rotation vs N_{ff}.

M = connection moment on the cyclic moment-rotation envelope corresponding to $\theta_{j\,eff}$ and
K_e = initial connection stiffness.

Equation 13 is related to the root mean cube of the response for a value of $c = -1/3$ where θ_j is taken as the peak amplitude for each cycle ($\theta_j = (\theta_{jmax} - \theta_{jmin})/2$).

It is generally difficult to identify the peaks and troughs in highly irregular or random events. Instead, if the points at each time step (Δt) in an analysis or experiment are used and the motion is harmonic, it can be shown that when $c = -1/3$

$$\theta_{j\,eff} = 1.33 \left(\frac{t_f}{\Delta t} \sum_{i=1}^{t_f/\Delta t} (\theta_j - \bar{\theta}_j)_i^3 \right)^{1/3} \tag{15}$$

where

$\bar{\theta}_j$ = mean rotation angle,
t_f = total time,
Δt = experimental time step.

A cyclic moment-rotation envelope curve can be deduced from a cyclic decremental test. The Menegotto-Pinto[9] equation is used herein (in a similar fashion to the monotonic envelope described in the companion paper[1]) to define the cyclic loading envelope as follows:

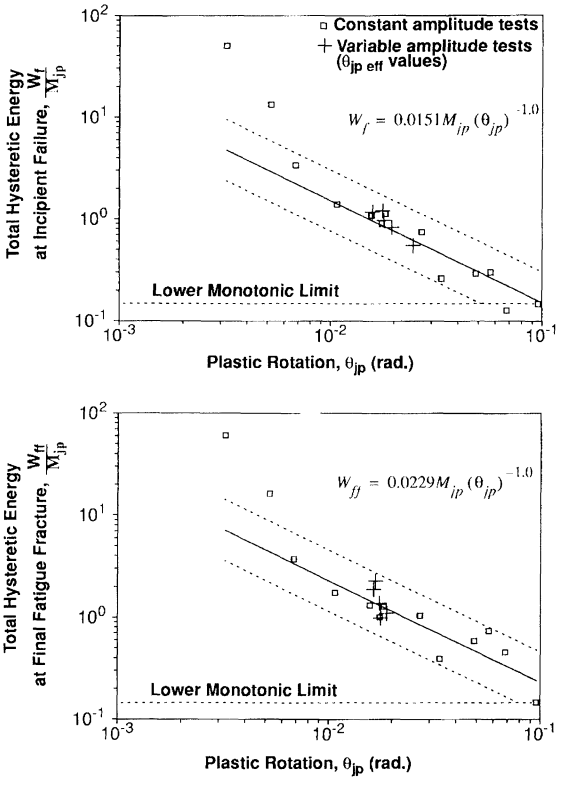

Fig. 8. (a) W_f vs plastic rotation. (b) W_{ff} vs plastic rotation.

Table 2.
Summary of Damage Analysis Results

Spec Id.	Experimental Results				Effective Amplitudes				Damage Rules	
					$\theta_{j\,eff}$		$\theta_{jp\,eff}$		Miner's Rule	Energy Based
	N_f	N_{ff}	W_f (kip-in)	W_{ff} (kip-in)	at N_f	at N_{ff}	at N_f	at N_{ff}	at N_f	at N_f
V_16	55	59	334.8	393.6	0.0181	0.0198	0.0158	0.0174	0.89	0.97
V_17	18	181	187.7	781.5	0.0274	0.0191	0.0246	0.0167	1.08	1.01
V_18	80	152	415.2	646.6	0.0202	0.0187	0.0177	0.0163	1.89	1.87
V_14	60	64	332.3	375.0	0.0204	0.0213	0.0179	0.0188	1.4	0.99
V_15	46	75	284.0	341.7	0.0220	0.0200	0.0195	0.0176	1.36	1.09

$$M = K_{je}\theta_j \left[Q + \frac{1-Q}{\left[1 + \left| \frac{K_{je}\theta_j}{M_{jp}} \right|^R \right]^{1/R}} \right] \qquad (16)$$

in which

K_{je} = the initial connection stiffness,
M_{jp} = connection mechanism moment which can be found graphically as the intersection of the two tangents forming the initial and plastic connection stiffnesses,
Q = ratio of plastic connection stiffness to initial connection stiffness,
$K_{jp} / K_{je}, R$ = a curvature parameter which determines the shape of the curve.

The parameters K_{je} = 120000 kip-in, M_{jp} = 200 kip-in, Q = 0.0415 and R = 2 were used to define the cyclic moment-rotation curve. Equivalent amplitude data points determined using Equation 14 are plotted in Figure 7(a) and 7(b) and compared with the constant amplitude tests at incipient failure as well as final fatigue failure. The equivalent plastic rotation amplitude ($\theta_{jp\,eff}$) values compare favorably with the constant amplitude test curves, and the data points are well within the upper and lower envelopes which were defined in the companion paper.[1]

ENERGY BASED MODELING

As noted earlier, in spite of its simplicity, Miner's Rule becomes quite cumbersome in the case of irregular loading histories where there may be several response frequencies occurring at once. Moreover, it is well known that metals have a memory of the past loading histories which may become significant with variable amplitude cyclic loading. Therefore, the loading sequence as well as the displacement amplitude can have an important effect on fatigue life. Miner's linear damage rule does not take this memory (sequence) effect into account.

The modified energy based Miner's Rule in Equation 8 can be rewritten to obtain the damage fraction as the ratio of incremental energy for the ith time-step to the current total energy. Again, in this case failure is assumed to occur when the summation of damage fractions equals or exceeds unity,

$$D_{wT} = \Sigma D_{wi} = \Sigma \frac{\delta w_i}{W_f(\theta_{jp\,eff})} \geq 1 \qquad (17)$$

where

δw_i = instantaneous incremental energy for the time interval (Δt) and is given by

$$\delta w_i = 0.5(M_i + M_{i-1})(\theta_{ji} - \theta_{ji-1}) \qquad (18)$$

where

M_i = experimentally observed moment at i^{th} time step,
W_f = total energy corresponding to the current effective plastic connection rotation $\theta_{jp\,eff}$, for the i^{th} time step.

In each case, the denominator in Equation 17 is updated at each time step using corresponding effective plastic connection rotation determined from Equation 15.

For the variable amplitude tests reported in Table 1, Figure 8(a) and 8(b) shows the total energy plotted vs. the effective plastic rotation $\theta_{jp\,eff}$ (determined from Equation 14) at incipient failure and fracture failure, respectively. These test results are compared with the constant amplitude relationships. It should be noted that the scatter in the experimental fatigue data poses problems in making predictions of failure using analytical relationships. However, most fatigue researchers consider experimental results to be of good quality if a failure prediction can be made within +100 percent or –50 percent of the line of best fit. These upper and lower bounds approximately correspond to 95 percentile range with a lognormal

distribution in experimental scatter. These bounds are plotted in Figures 7 and 8.

Figures 9 through 13 show the rotation and moment time-histories for the test specimens. The effective connection rotation ($\theta_{j\,eff}$) is also plotted on the connection rotation graph in order to demonstrate the sequence effects on the connection behavior. The accumulation of damage for both Miner's Rule and the proposed energy based damage model are also shown in these figures. For the latter model damage at time t is computed by substituting Equation 18 in the numerator and Equation 5 for the value of $\theta_{jp\,eff}$ in the denominator,

$$D(t) = \sum_{i=1}^{t} \left[\left(\frac{M_i + M_{i-1}}{2} \right) (\theta_{ji} - \theta_{ji-1}) \frac{\theta_{jpi}}{0.0151 M_{jp}} \right] \qquad (19)$$

where

$\theta_{jp\,i}$ is given by Equation 14 and
i = data point number.

It can be observed from Table 2 and Figures 10 and 11 that for high-low step tests, both models produce a similar type of damage accumulation, i.e., the damage rate as well as the cumulative damage at N_f and N_{ff} are similar. However, for the other test specimens the damage accumulation patterns are different for the two models, with the energy based model giving improved results for both N_f and N_{ff}. It appears from the cumulative damage plots that the energy based model is more capable of reflecting the effect of past rotation histories, by using the effective plastic rotation amplitude. Moreover, the area within the moment-rotation loops (energy dissipated) is directly affected by the sequence of loading which in turn is reflected in the rate of damage accumulation.

The results demonstrate that the concept of converting variable amplitude history into an equivalent constant amplitude history appears viable for at least the investigated class of semi-rigid connections. The advantage of employing an energy based model is that memory effects can be taken into account by using the effective plastic rotation in determining the total energy till incipient failure, W_f. The value of W_f at a certain plastic rotation amplitude can be calculated using a low-cycle fatigue relationship in the form of Equation 3.

Krawinkler and Zohrei[4] used an implicit form of Miner's Rule of linear damage accumulation in conjunction with Equation 1 using an exponent of –0.5 to –0.67 for welded steel connections. Mean rotation effects were ignored in the formulation whereas, in the present study, linear damage accumulation has been extended using energy absorption concepts. Morever, mean rotation effects have been taken into account by numerically integrating the dissipated energy as mentioned previously.

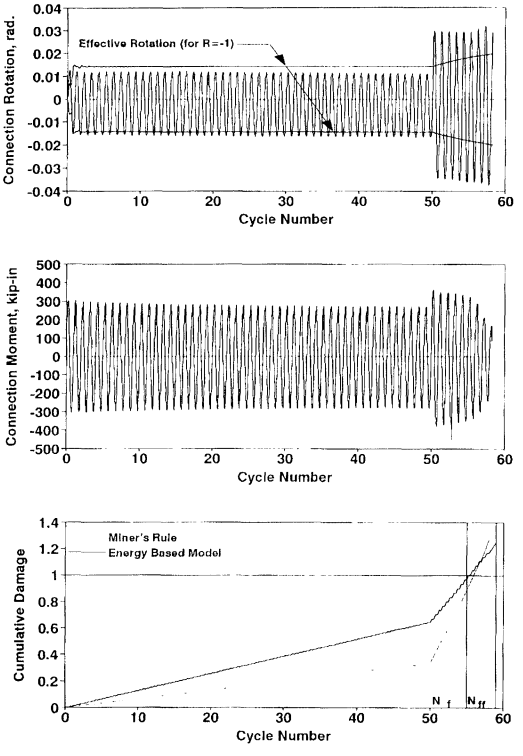

Fig. 9. Damage analysis results, specimen V_16.

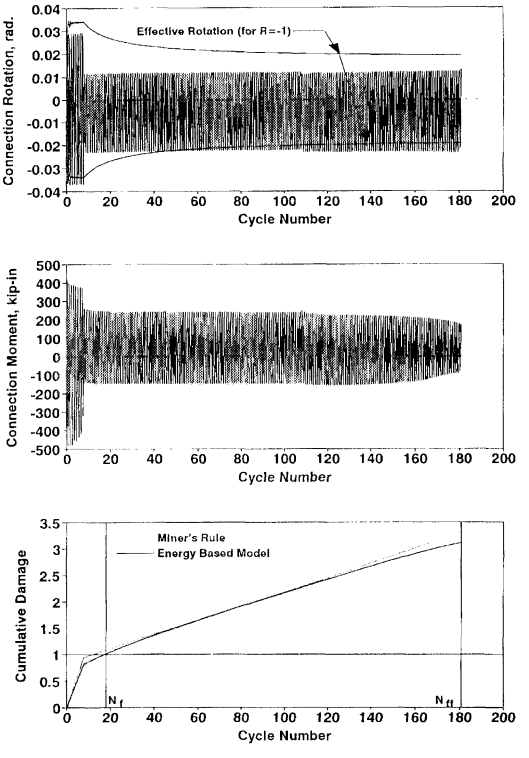

Fig. 10. Damage analysis results, specimen V_17.

CONCLUDING REMARKS

The purpose of the investigation described in this paper was to develop an efficient predictive low-cycle fatigue-life model that avoids the pitfalls of the present commonly used models. The proposed energy-based fatigue damage model is particularly well suited to predicting incipient failure of top-and-seat angle connections subjected to variable amplitude load histories. Miner's model for linear damage accumulation can be extended using energy absorption concepts. This approach explicitly accounts for path dependency in variable amplitude histories.

The energy based low-cycle fatigue damage model proposed in this study was validated by the variable amplitude test results on top-and-seat angle connections. This validation is over the range of amplitudes expected in the response of relatively weak steel structures in an extreme earthquake excitation ($\theta_j < 0.04$ radians). This model monitors the incremental damage via hysteretic energy absorption. An effective plastic rotation concept was introduced in the cumulative damage model. This was found to be a convenient way of characterizing the energy capacity under both constant and variable amplitude histories since cyclic energy dissipation mainly depends on the plastic rotation. Sequence effects are taken into account by numerically integrating the dissipated energy and revising the denominator of the damage fraction at each time step. For analysis with real earthquake time histories, cycle counting as required by Miner's Rule may become quite cumbersome. Hence, an important advantage of the energy-based approach is that no cycle counting is necessary for damage evaluation purposes.

However, although the model is general in nature, it should be validated for different top-and-seat angle bolting geometries. In order for the model to be utilized for different types of steel connections, such as welded connections or connections with web cleats, further tests should be conducted to calibrate Equations 1 to 6.

ACKNOWLEDGMENT

Specimens were donated by Tom Latona of Buffalo Structural Steel Corporation. Partial financial support was provided by the National Center for Earthquake Research (NCEER) headquartered at SUNY at Buffalo. The help of NCEER technicians Mark Pitman and Dan Walch who assisted in the experimental study is gratefully acknowledged.

REFERENCES

1. Mander, J. B., Chen, S. S., Pekcan, G., "Low-Cycle Fatigue Behavior of Semi-Rigid Top-and-Seat Angle Connections," *Engineering Journal*, AISC, in press.
2. Palmgren, A., "Durability of Ball Bearings," *ZVDI*, Vol. 68, No. 14, 1924, pp. 339–341 (in German).
3. Miner, M. A., "Cumulative Damage in Fatigue," *Trans.*

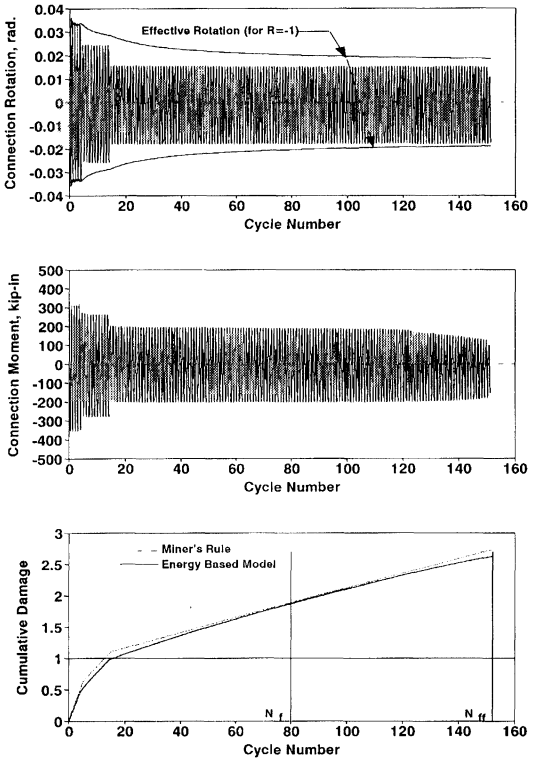

Fig. 11. Damage analysis results, specimen V_18.

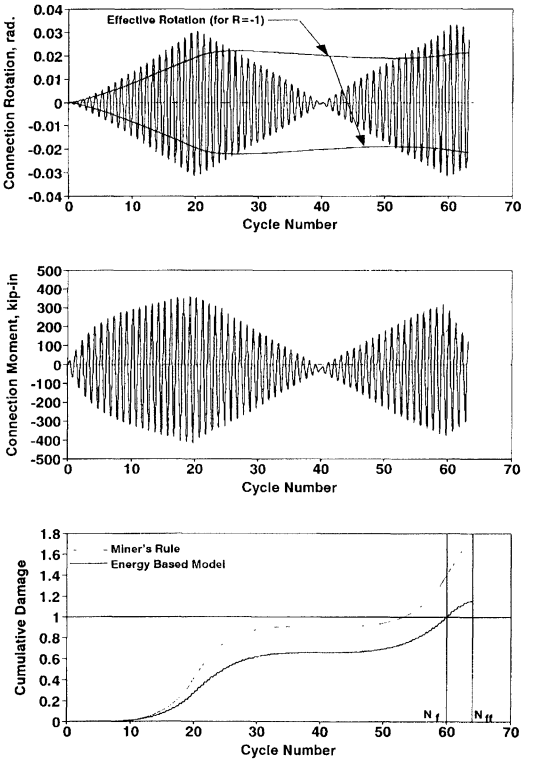

Fig. 12. Damage analysis results, specimen V_14.

ASME, Journal of Applied Mechanics, Vol. 67, 1945, pp. A159–A164.

4. Krawinkler, H., and Zohrei, M., "Cumulative Damage in Steel Structures Subjected to Earthquake Ground Motions," *Journal of Computers and Structures*, Vol. 16, No. 1–4, 1983, pp.531–541.
5. Matsuishi, M. and Endo, T., "Fatigue of Metals Subjected to Varying Stress," paper presented to *Japan Society of Mechanical Engineers*, Fukuoka, March 1968.
6. Coffin, L. F., Jr., "A Study of the Effects of Cyclic Thermal Stresses on a Ductile Metal," *Trans. ASME*, Vol. 76, August 1954, pp. 931–950.
7. Manson, S. S., "Behavior of Materials Under Conditions of Thermal Stress," *Heat Transfer Symposium, University of Michigan Engineering Research Institute*, 1953, pp. 9–75.
8. Koh, S. K., Stephen, R. I., "Mean Stress Effects on Low-Cycle Fatigue for a High Strength Steel," *Fatigue Fracture of Engineering Materials and Structure*, Vol. 14, No. 4, pp. 413–428, 1991.
9. Menegotto, M. and Pinto, P. E., "Method of Analysis for Cyclically Loaded Reinforced Concrete Plane Frames Including Changes in Geometry and Non-Elastic Behavior of Elements Under Combined Normal Forces and Bending," *IABSE Symposium on the Resistance and Ultimate Deformability of Structures Acted on by Well-Defined Repeated Loads*, Lisbon 1973.

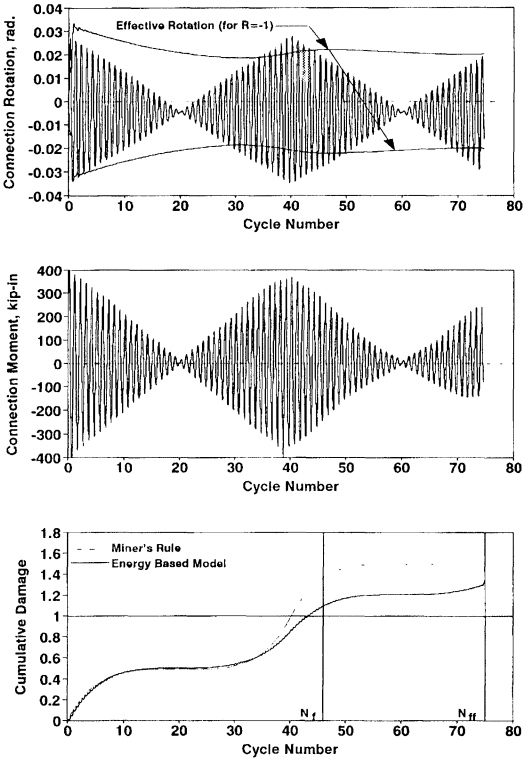

Fig. 13. Damage analysis results, specimen V_15.